Available online at www.sciencedirect.com
SCIENCE DIRECT®
Deep-Sea Research I 51 (2004) 129–151
DEEP-SEA RESEARCH PART I
www.elsevier.com/locate/dsr

Instrument and Methods

What you see is not what you catch: a comparison of concurrently collected net, Optical Plankton Counter, and Shadowed Image Particle Profiling Evaluation Recorder data from the northeast Gulf of Mexico

Andrew Remsen[a,*], Thomas L. Hopkins[a], Scott Samson[b]

[a] University of South Florida College of Marine Science, 140 7th Avenue S., St. Petersburg, FL 33701, USA
[b] Center for Ocean Technology, University of South Florida, 140 7th Avenue S., St. Petersburg, FL 33701, USA

Received 18 February 2003; received in revised form 15 September 2003; accepted 15 September 2003

Abstract

Zooplankton and suspended particles were sampled in the upper 100 m of the Gulf of Mexico with the High Resolution Sampler. This towed-platform can concurrently sample zooplankton with plankton nets, an Optical Plankton Counter (OPC) and the Shadowed Image Particle Profiling and Evaluation Recorder (SIPPER), a zooplankton imaging system. This allowed for direct comparison of mesozooplankton abundance, biomass, taxonomic composition and size distributions between simultaneously collected net samples, OPC data, and digital imagery. While the net data were numerically and taxonomically similar to that of previous studies in the region, analysis of the SIPPER imagery revealed that nets significantly underestimated larvacean, doliolid, protoctist and cnidarian/ctenophore abundance by 300%, 379%, 522% and 1200%, respectively. The inefficiency of the nets in sampling the fragile and gelatinous zooplankton groups led to a dry-weight biomass estimate less than half that of the SIPPER total and suggests that this component of the zooplankton assemblage is more important than previously determined for this region. Additionally, using the SIPPER data we determined that more than 29% of all mesozooplankton-sized particles occurred within 4 mm of another particle and therefore would not be separately counted by the OPC. This suggests that coincident counting is a major problem for the OPC even at the low zooplankton abundances encountered in low latitude oligotrophic systems like the Gulf. Furthermore, we found that the colonial cyanobacterium *Trichodesmium* was the most abundant recognizable organism in the SIPPER dataset, while it was difficult to quantify with the nets. For these reasons, the traditional method of using net samples to ground truth OPC data would not be adequate in describing the particle assemblage described here. Consequently we suggest that in situ imaging sensors be included in any comprehensive study of mesozooplankton.

Keywords: Zooplankton; Plankton-collecting devices; Samplers; Imaging; Optics; Abundance; Biomass; Vertical distribution; OPC; USA; Florida; Gulf of Mexico; 27°N 86°W

*Corresponding author. Tel.: +1-727-553-3970; fax: +1-727-553-1189.
E-mail address: aremsen@marine.usf.edu (A. Remsen).

0967-0637/$ - see front matter © 2003 Elsevier Ltd. All rights reserved.
doi:10.1016/j.dsr.2003.09.008

1. Introduction

Zooplankton are key mediators of particle flux, fisheries recruitment and biomass production within the world oceans (Lenz, 2000). Information on their abundance and distribution in space and time are required to accurately predict their contribution to these processes. Field observations of zooplankton indicate that they operate along a continuum of spatial and temporal scales leading to heterogeneous or "patchy" distribution patterns (Haury et al., 1977; Omori and Hamner, 1982; Gallienne et al., 2001). Traditional methods such as plankton nets, pumps and bottles are limited in sampling zooplankton over the entire distribution spectrum, especially at the fine scale (meters to hundreds of meters, seconds to hours) because of their integrative nature and the time consuming task of analyzing individual zooplankton samples. Additionally, a significant fraction may be undersampled by plankton nets because of extrusion through the net mesh, hang-up within the net, and destruction of fragile forms such as gelatinous zooplankton when physically captured (Gallienne and Robins, 2001; Halliday et al., 2001; Hopcroft et al., 2001; Warren et al., 2001).

To address these limitations, alternative instruments for sampling zooplankton in situ have been developed over the last 20 years (Schulze et al., 1992; Skjoldal et al., 2000; Wiebe and Benfield, 2003). These new devices provide the increased spatial and temporal resolution necessary to study the coupling between physical processes and zooplankton distribution patterns and for modeling zooplankton population and tropho-dynamics. One of the most widely used of these new instruments is the Optical Plankton Counter (OPC), with approximately one hundred units in use throughout the world (Zhou and Tande, 2002). The OPC provides quantitative measurements of abundance and size of mesozooplankton-sized particles (250 μm–2 cm) and can be deployed from a diverse array of platforms (Foote, 2000). However, the taxonomic resolution of the OPC is limited except in low diversity assemblages where separable peaks in a OPC generated size distribution might be attributable to a specific species or developmental stage (Herman, 1992). Consequently, the OPC is most often used to complement net data by providing high-resolution information on the spatial distribution patterns of the net-identified zooplankton. While many investigators have found rough agreement between net counts and OPC estimates of zooplankton abundance (Foote, 2000; Zhou and Tande, 2002), there have been instances where the OPC and net abundance estimates have differed significantly (Grant et al., 2000; Halliday et al., 2001; Sutton et al., 2001). These differences have been attributed to extrusion of zooplankton through the plankton net mesh, counting of detrital aggregates and or large phytoplankton colonies, and coincident counting where the OPC counts multiple particles in the light path as a single larger particle (Woodd-Walker et al., 2000; Zhang et al., 2000; Halliday et al., 2001).

Advances in zooplankton imaging technology could help make sense of these conflicting results. Results from instruments such as the Video Plankton Recorder (VPR, Davis et al., 1992) and the Shadowed Image Particle Profiling and Evaluation Recorder (SIPPER, Samson et al., 2001) indicate that they can provide both high quality taxonomic information and high resolution in the temporal and spatial domains. Previous comparisons between the VPR and nets have indicated that they describe similar distributions for abundant zooplankton groups (Benfield et al., 1996; Gallager et al., 1996), are more effective at sampling fragile and gelatinous forms than nets (Norrbin et al., 1996; Dennett et al., 2002), and can assess the contribution of detrital aggregates or "marine snow" to particles in the mesozooplankton size range (Ashjian et al., 2001).

This paper compares the abundance and size distribution of mesozooplankton and suspended particles sampled by nets and the OPC against data concurrently collected by the SIPPER in offshore waters of the Gulf of Mexico. We hypothesized that the SIPPER should image all particles within the mesozooplankton size range that would be resolvable by either the net or the OPC and act as an independent "ground truth" against the other two sampling systems. The composition of the mesozooplankton assemblage

sampled by the SIPPER and plankton nets was then compared.

2. Methods

Zooplankton were sampled at a station in the eastern Gulf of Mexico (27°N 86°W, 3 km water depth) with the High Resolution Sampler (HRS), a comprehensive towed marine particle analysis platform (Fig. 1; see Sutton et al., 2001 for a full description). The HRS samples zooplankton through a square 9.6 cm sampling tube (92.16 cm^2 mouth area) leading to a, 20-position cod-end net carousel fitted with 162 μm plankton nets. The nets have an open filtering area to mouth area ratio of 11:1 and the aluminum sampling tube precludes retention of organisms. Mounted inline with the sampling tube was the SIPPER zooplankton-imaging sensor. The sampling tube projects past the frame of the HRS and has a knife-edge to minimize any pressure wave that might develop in front of the aperture to reduce possible avoidance of the sampler by zooplankton. An OPC with a rectangular 2×22 cm sampling aperture (44 cm^2 mouth area) was mounted within the frame of the HRS and a half-meter below the sampling tube. The OPC was positioned so that it would sample water that was not influenced by the frame of the HRS.

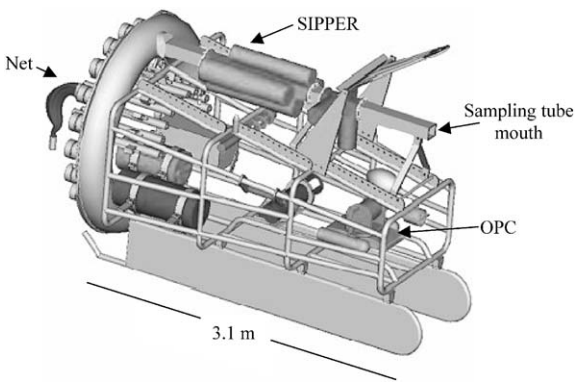

Fig. 1. Schematic of the USF HRS and its associated zooplankton sampling systems. Only one net is shown attached at the carousel to reduce confusion in the figure.

Both net and electronic zooplankton sampling are computer controlled on-deck via a custom designed software interface such that new SIPPER and OPC files are created and the sensors begin sampling when a net is triggered open. When a particular net run is completed and ordered closed, the files corresponding to that net sample are also closed, thereby creating two independent samples that can be compared against the net sample. Environmental and diagnostic information (CTD, fluorometer, transmissometer, inclinometer, and flow-meter data) are continuously recorded on a separate HRS data file.

A single deployment sampling 10 discrete depths (10–100 m in 10 m increments) beginning two hours after local sunset on July 21, 2000, was chosen for this study. Each depth was sampled for 10 min. The SIPPER and the net system both collect zooplankton through the sampling tube at the front of the HRS and therefore sample the exact same volume of water. 37.9 m^3 of water was sampled by these two systems for this study, averaging 3.79 ($\pm$0.18) m^3 per depth stratum. The OPC, which was situated below and slightly aft of the HRS sampling tube, has a sampling aperture approximately half that of the other two systems, and filtered a total of 18.39 m^3 of seawater, averaging 1.84 ($\pm$0.09) m^3 per depth stratum. Tow speed was determined with a calibrated flow meter (TSK Inc.) mounted at the front of the sampler. It registered a near constant tow-speed of 0.75 m s^{-1}. Inclinometer data indicated that the HRS maintained a near-perfect horizontal attitude at each depth stratum.

2.1. Net sample treatment

Zooplankton collected in the nets were fixed immediately in 5% v:v buffered formalin upon recovery of the sampler and stored for later analysis in the laboratory. Net samples were split into subsamples, when necessary, with a Motoda splitter for analysis of approximately 1000 individual organisms per sample. Identifications were carried out to species when possible for copepods and to major group for the other taxa with a dissecting microscope. The cyanobacteria *Trichodesmium* was noted if present but was not

enumerated, as it tends to be difficult to wash off the net mesh making quantitative analysis difficult.

Zooplankton were measured to total length by methods described in Hopkins (1981). Equivalent spherical diameter (ESD) was calculated for individuals of each taxon with Optimas (Media Cybernetics, version 6.5) image analysis software and a video camera connected to the microscope for comparison with OPC and SIPPER size measurements. Optimas determines ESD by measuring the area of an object and then calculating the diameter of a sphere with the same area. Regressions for calculating ESD from total lengths for each taxon were then calculated and applied to each net sample. Sample biovolume (SBV) was calculated for each sensor according to the equation

$$\mathrm{SBV} = k\left[\sum_{i=1}^{n}\frac{\pi}{6}(\mathrm{ESD}_i)^3\right], \quad (1)$$

where k is the sub-sample ratio, n the number of individuals, and ESD_i the ESD of the ith individual (Labat et al., 2002). Biomass for net and SIPPER samples was calculated from regressions determined for zooplankton from the Gulf of Mexico by our laboratory (Table 1).

2.2. SIPPER data analysis

The SIPPER is a continuously imaging zooplankton sensor that records two dimensional, high resolution images of zooplankton and other suspended particles prior to sampling by the HRS plankton nets (for a full description of SIPPER, see Samson et al., 2001). The SIPPER works by projecting a collimated laser light sheet perpendicular to seawater flow through the sampling tube of the HRS and continuously imaging the outlines and shadows of particles as they pass through the sheet with two line-scan camera systems mounted orthogonal to each other. In this manner, pairs of digital images are created for each particle passing through the sensor. Because zooplankton will be randomly oriented as they pass through SIPPER, the use of two orthogonally mounted cameras significantly increases the possibility that at least one camera will capture an image of a zooplankter in a recognizable orientation. Line-scan cameras build an image one line at a time, and because the particle flow through the SIPPER/net sampling

Table 1
Dry weight biomass regressions from oceanic waters of the Gulf of Mexico

Group	Dry weight regressions (mg DW)	Correlation (r^2)	Notes	
Copepod	$DW = 0.0085(ML)^{3.1007}$	0.988	ML = metasomal length	Combination of 38 copepod taxa in the NE Gulf of Mexico
Chaetognath	$DW = 0.0002(TL)^{3.1612}$	0.971		
Cnidaria	$DW = 0.0029(ESD)^{2.2851}$	0.868		
Decapod and euphausiid	$DW = 0.001(TL)^{3.1331}$	0.977		
Doliolid and salp	$DW = 0.0108(TL)^{1.6307}$	0.986		
Larvacean	$DW = 0.0164(HL)^{2.0922}$	0.995	HL = head length	
Meroplankton	$DW = 0.0041(ESD)^{2.31}$	0.881		Mostly echinoderm bipinnaria and plutei
Mollusc	$DW = .0296(ESD)^{1.5646}$	0.878		Mostly pteropods and some heteropods
Other crustaceans	$DW = 0.0505(TL)^{1.8223}$	0.982		Mostly ostracods and some amphipods
Polychaete	$DW = 0.0091(TL)^{1.801}$	0.977		Combination of unid. polychaetes and *Tomopteris* sp.
Siphonophore	$DW = 0.0088(TL)^{0.0414}$	0.981		

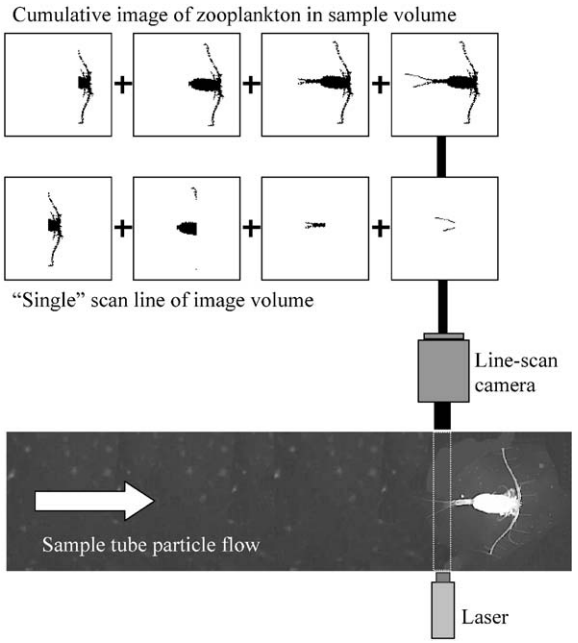

Fig. 2. Diagram illustrating the general concept of the SIPPER line-scan camera system. A cumulative image of the sample volume is built of many individual single scan lines. In this figure, multiple scan lines are included in the "single scan line" frames in order to minimize the number of single scan line frames illustrated.

tube is unidirectional, each particle can only be imaged once. Fig. 2 demonstrates the concept of a single line-scan camera system. Real time thresholding of the image volume and final storage of the image data as black and white bitmap images improves data storage and reduces post-processing steps such as edge detection.

Image resolution is determined by the line scan camera pixel array size in one dimension (in this case 9.6 cm divided by 2048 pixels in the camera array allows for 47 μm resolution) and the flow speed through the sample tube divided by the line scan rate of the camera system in the other (in this case $\sim 0.75\,\mathrm{m\,s^{-1}}$ divided by 15,000 line scans a second allows for an average pixel dimension of 50 μm). Therefore, pixels used for SIPPER imaging were almost perfectly square with dimensions of 47×50 μm. This was confirmed by comparing the size of large unique organisms from the SIPPER dataset with the actual organisms from the concurrent net sample.

Because the SIPPER is a high-resolution continuously imaging sensor, a significant amount of data is generated and recorded every second. Black and white image data were recorded at approximately 8 megabytes $\mathrm{s^{-1}}$, with each raw SIPPPER file averaging 4.8 gigabytes total. Fortunately, SIPPER data is perfectly suited for run-length encoding compression algorithms whereby long runs of identical binary data can be represented by much shorter binary descriptions resulting in significant data storage savings (up to $277\times$). When decompressed, each SIPPER file can be thought of as a "strip chart" the length of each sampling run (~ 0.5 km) and a width of 9.6 cm with images of every organism and particle that passed through the sample tube recorded in the approximate spatial distribution that existed in situ but expressed in two dimensions.

Custom region-of-interest (ROI) extraction software developed using LabWindows/CVI (National Instruments) was used to detect and create bitmaps of zooplankton and particles of a user-defined size and greater. The routine first divides the SIPPER data into a number of convenient, 2048×2048 pixel "frames", each of which is equivalent to approximately 1/7th of a second of sampling or 10.24 cm (Fig. 3). ROIs were then located in each frame and extracted. For this study, ROIs were extracted that were larger than 250 μm ESD. A preprocessing digital dilation step ensured that organisms and particles with non-contiguous boundaries were included in the ROI extraction but would still be counted as a single particle. This ensured that almost all particles greater than 250 μm ESD were extracted from the raw SIPPER file.

Extracted, non-processed particle images were then viewed with a thumbnail browsing program (Thumbs Plus, Cerious Software). Recognizable plankton images were manually classified into 13 groups (Fig. 4) and unrecognizable particles were placed into a separate unidentified class. Marine snow was included in the unidentified class. *Trichodesmium* colonies were included as a plankton class because of their high abundance in the SIPPER dataset and large individual size. Because

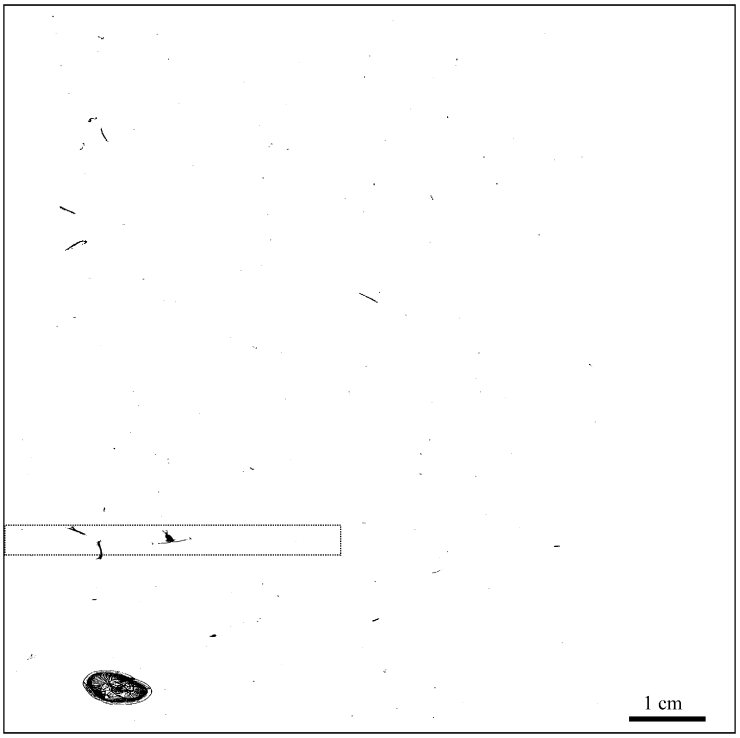

Fig. 3. 2048 × 2048 pixel frame illustrating the large sampling area of SIPPER and its image quality. The dashed line represents the dimensions of the "pseudovolume" used to estimate OPC coincidence (4.6 × 9.6 × 0.4 cm). Scale bar is equivalent to 1 cm.

of the high diversity of the zooplankton assemblage in the deepwater Gulf of Mexico (e.g. Ortner et al., 1989 identified 133 separate zooplankton species) we did not attempt to use SIPPER to identify organisms to species even though some species with characteristic features were easily recognized. ROIs of organisms that spanned multiple frames were identified manually and spliced back together after the extraction routine was ended. Each separate class was then analyzed with Optimas running a custom macro that collected size and morphological information from each ROI including ESD. The location of each ROI within the SIPPER sampling transect was recorded on a separate data file. Locations were then checked against each other to ensure that no particle was counted more than once. SIPPER data were not sub-sampled. Because of the large number of images that had to be manually classified, only images from one of the two orthogonal views were used for this study.

2.3. OPC data analysis

A detailed explanation of the design and operation of the OPC is found in Herman (1992). Basically the OPC measures the amount of light blocked by the area of a particle as it passes through a collimated light sheet between the transmitter and receiver. The blocked light signal is digitized and converted into a size measurement in the form of an ESD. The OPC is capable of resolving particles 250 μm ESD and greater in size (Herman, 1988, 1992), but is vulnerable to coincident counting at high particle concentrations (undercounting multiple particles that pass through collimated light sheet at the same time) and has difficulty accurately describing the size of translucent organisms (Zhang et al., 2000; Grant et al., 2000). OPC determined particle size data were binned into 100 μm ESD groups (300–5000 μm) for comparison with the net and SIPPER zooplankton data.

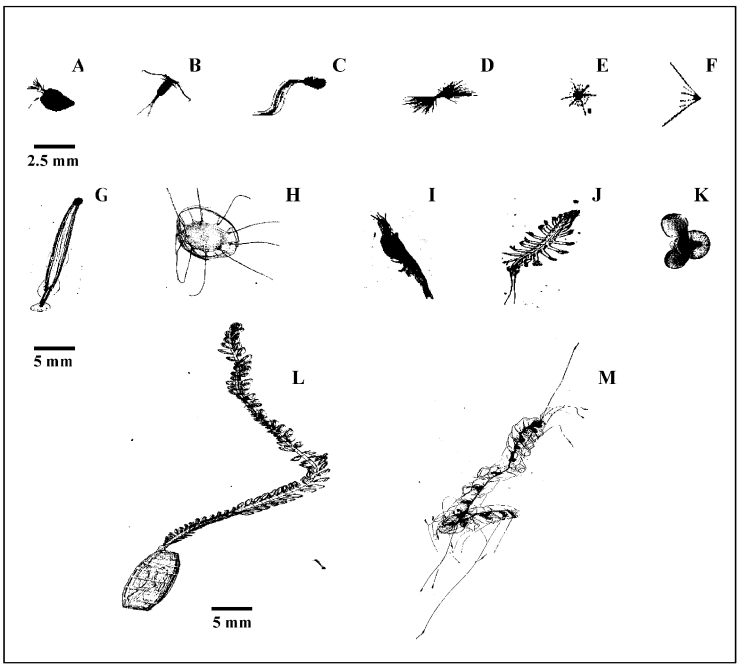

Fig. 4. Representative SIPPER images of the 13 enumerated plankton groups. Groups A–F are from left to right, with group code in parentheses: (A) other crustaceans (Crus), (B) copepods (Cope), (C) larvaceans (Larv), (D) *Trichodesmium* sp. (Tric), (E) protoctists (Prot), (F) echinoderm larvae (Echi). Scale bar for these groups is equivalent to 2.5 mm. Groups G–M are, from left to right: (G) chaetognaths (Chae), (H) cnidarians and ctenophores (Cnid), (I) euphausiids and decapods (Euph), (J) Polychaetes (Poly), (K) Mollusks (Moll), (L) other tunicates (Tuni) and (M) siphonophores (Siph). Scale bar for these groups is equivalent to 5 mm.

3. Results

3.1. Hydrographic conditions

Summertime conditions in the northeast Gulf of Mexico are usually stable with the exception of quasi-annual intrusions of the Loop Current and associated eddies (Maul and Vukovich, 1993; Müller-Karger, 2000) and even rarer incursions of low salinity surface plumes from the Mississippi River outflow (Müller-Karger et al., 1991; Müller-Karger, 2000) that might influence the zooplankton assemblage (Ortner et al., 1995). Temperature and salinity profiles collected during this study (Fig. 5) indicated the water being sampled as Gulf Common Water (GCW, Vidal et al., 1994). This is differentiated from Subtropical Underwater (SUW) being transported by the Loop Current by the depth of the 22°C isotherm. In GCW the 22°C isotherm is found between 50 and 100 m whereas in the Loop Current it is found below 150 m (Austin and Jones, 1974). The seasonal thermocline was located between 25 and 30 m depth. Salinity profiles (Fig. 5) and satellite data indicated no influence from the Mississippi River. The deep chlorophyll maximum (DCM) was at approximately 65 m near the salinity maximum, and there was very low chlorophyll biomass throughout the rest of the epipelagic zone based on both in situ fluorescence and extracted chlorophyll (Fig. 5).

3.2. Mesozooplankton and mesozooplankton sized particle abundance

The vertical distribution pattern of mesozooplankton and mesozooplankton-sized particles was described similarly by all three sampling methods (Fig. 6). There was a peak in abundance at 10 m and a secondary maximum at 40 m. The

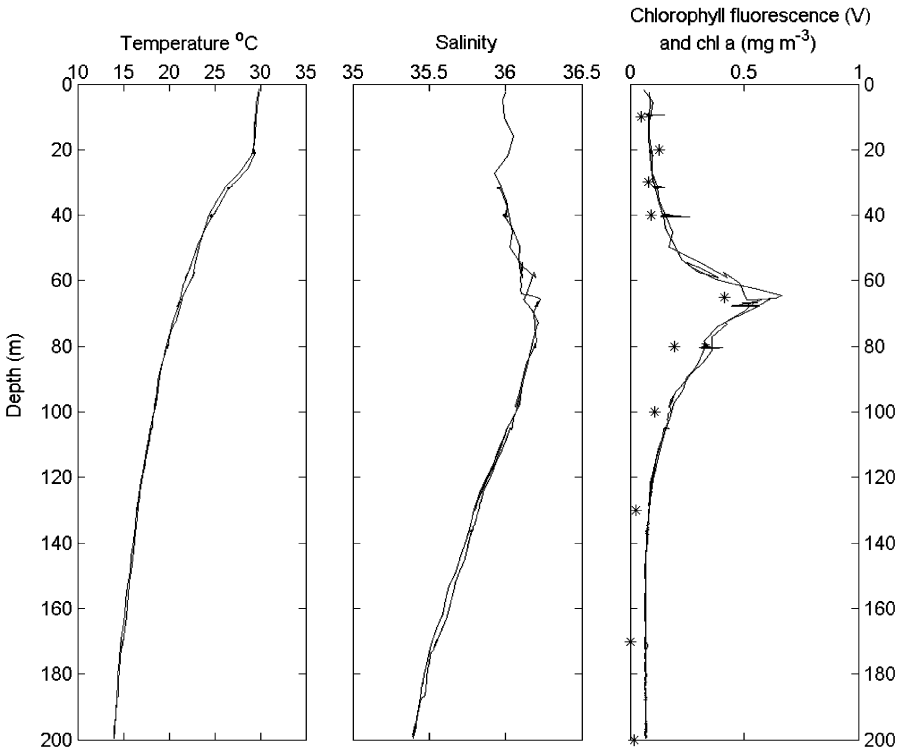

Fig. 5. Temperature, salinity, fluorescence and extracted chlorophyll (denoted by ∗) profiles (0–200 m) from the study site.

major difference was in the total number of particles sampled by each method. The SIPPER recorded the highest numbers of mesozooplankton-sized particles at all depths sampled when compared against the results of the nets and the OPC. The SIPPER data were separated into two abundance estimates: (1) total number of extracted ROI images with a greater than 250 μm ESD "particle" (SIPPER total) and (2) those ROIs that could be identified as planktic organisms (SIPPER i.d.). A total of 174,699 SIPPER ROIs were extracted and manually examined from the 100 min of SIPPER data. Most of these images contained unrecognizable particles and only 28% of the total (48,931 plankton images) could be classified into one of the 13 plankton groups. The proportion of SIPPER i.d. to SIPPER total ranged from 41% at 10 m to 17% at 100 m (Table 2). Plankton net estimates of mesozooplankton abundance were the lowest at each depth sampled relative to the other sampling methods. Net counts on average equaled only 13% of the SIPPER total, 24% of the OPC total and 49% of SIPPER identified plankton abundance.

The OPC consistently sampled approximately half the number of particles that the SIPPER imaged at all depths.

3.3. OPC abundance correction and coincidence frequency

Assuming particles were randomly distributed within the water column, Sprules et al. (1992) derived a formula describing the probability of two or more particles occurring within the sampling beam of the OPC at the same time given a known particle concentration. They determined that coincidence would be a significant source of error for all but the lowest zooplankton densities. To determine if coincidence was responsible for the low OPC counts relative to the SIPPER total, we modified the formula of

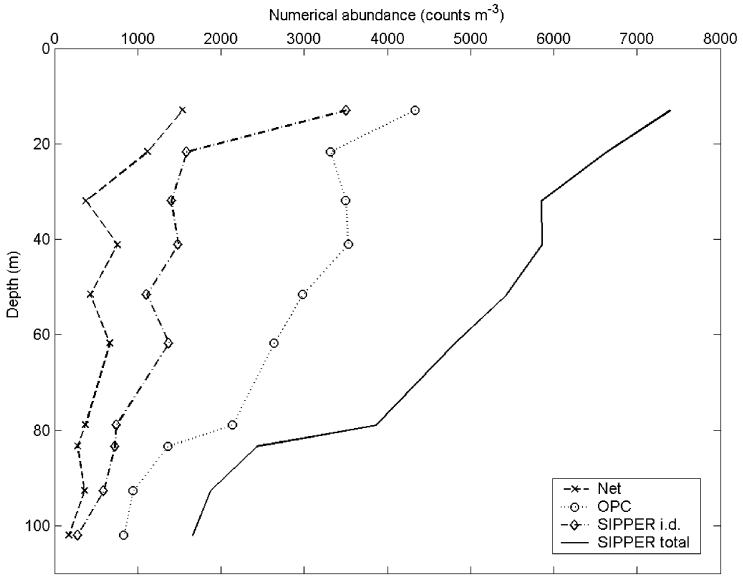

Fig. 6. Numerical abundance estimates of the three zooplankton sampling methods. SIPPER abundances are broken down into total number of ROIs with a larger than 250 μm particle (SIPPER total) and those imaged particles that could be classified into one of the 13 plankton groups (SIPPER i.d.). All estimates have been normalized to volume filtered.

Table 2
Abundance (number m^{-3}) of mesozooplankton sized particles as estimated by the 162 μm net system, SIPPER and the OPC

Depth (m)	Net counts	SIPPER total	SIPPER identified images	OPC counts	Net counts/ SIPPER total (%)	SIPPER identified/ SIPPER total (%)	OPC counts/ SIPPER total (%)
10	1537	7397	3508	4335	21	47	59
20	1117	6634	1591	3320	17	24	50
30	374	5849	1404	3497	6	24	60
40	756	5855	1487	3529	13	25	60
50	431	5428	1106	2983	8	20	55
60	664	4811	1372	2640	14	29	55
70	371	3864	742	2139	10	19	55
80	279	2428	727	1365	11	30	56
90	359	1877	591	942	19	31	50
100	171	1657	276	831	10	17	50

SIPPER counts are split into total ROIs with a greater than 250 μm ESD particle within it, and those images that could be classified into one of the 13 plankton groups. Performance of the net system, SIPPER identified plankton and the OPC are all compared against the SIPPER total.

Woodd-Walker et al. (2000) using SIPPER total counts normalized to volume sampled as the known concentration of OPC detectable particles in the OPC light beam. The average number of particles in the OPC beam (μ) is determined by

$$\mu = C \times V, \tag{2}$$

where C was the concentration of particles greater than 250 μm in the SIPPER total for each depth and V was the volume of the OPC beam (220 mm × 20 mm × 4 mm or 17.6 ml). The average number of particles recorded by the OPC (av. no.) is calculated by the equation:

$$\text{OPC av. no.} = 1 - e^{-\mu} \quad (3)$$

(Woodd-Walker et al., 2000). The coincidence factor can then be calculated by dividing the average number of particles in the OPC beam by the average number of particles recorded by the OPC (coincidence factor = μ/OPC av. no). For this study, the coincidence factor ranged from 1.01 to 1.06 indicating that coincidence should have been a rare occurrence within the OPC if the particles were randomly distributed at the concentrations sampled by SIPPER (1–8 particles l^{-1}).

To investigate further, we created a "pseudovolume" within the SIPPER image dataset equivalent to the volume sampled by the OPC at any one instant. Because the sampling area of the SIPPER is approximately twice that of the OPC and of a different geometry, we used a sub-sample of the SIPPER imaging window that was 4.6 cm × 9.6 cm × 0.4 cm to create a sampling volume of 17.6 ml, equivalent to that of the OPC. We calculated the distance between each particle from its neighbors within the "pseudovolume" to determine which particles would be affected by coincident counting (this can be visualized in Fig. 3, where a copepod and two *Trichodesmium* colonies occupy the dotted box representing the "pseudovolume" dimensions), if the SIPPER were to sense particles like the OPC. On average, 29% of SIPPER imaged particles of OPC detectable size had a neighbor closer than 4 mm and therefore would not be individually counted by the OPC (Table 3). By correcting for the estimated coincidence frequency, OPC abundance values were recalculated and agreed more closely with the SIPPER total. The large number of close-together particles suggests that their distribution was not random.

3.4. Size frequency

The cumulative size-frequency distributions of the three sampling methods demonstrated large differences in sampling performance (Fig. 7). While each sampling method was able to discern the same exponential decrease in abundance with increasing size, the SIPPER was able to detect far more particles than either the net or OPC for a given size class. Much of the discrepancy between the SIPPER total and SIPPER i.d. abundances could be attributed to the large number of less than 0.5 mm ESD particles that could not be identified. This was most likely due both to the large numbers of small-suspended particulates in the water column and also the minimum size resolution of identifiable objects in the SIPPER dataset. While the SIPPER can image very small

Table 3
OPC normalized particle abundance, theoretical coincidence factor, SIPPER estimated coincidence percentage, count loss and corrected OPC particle abundance

Depth (m)	OPC counts m^{-3}	Coincidence factor	SIPPER-estimated coincidence (%)	Counts lost to coincidence	Corrected OPC counts m^{-3}
10	4335	1.06	33.6	1458	5793
20	3320	1.05	38.3	1270	4591
30	3497	1.05	33.0	1154	4651
40	3529	1.05	30.1	1063	4591
50	2983	1.04	27.1	808	3791
60	2640	1.04	23.6	624	3264
70	2139	1.03	24.7	539	2668
80	1365	1.02	21.9	299	1664
90	942	1.02	22.2	209	1152
100	831	1.01	23.3	194	1025

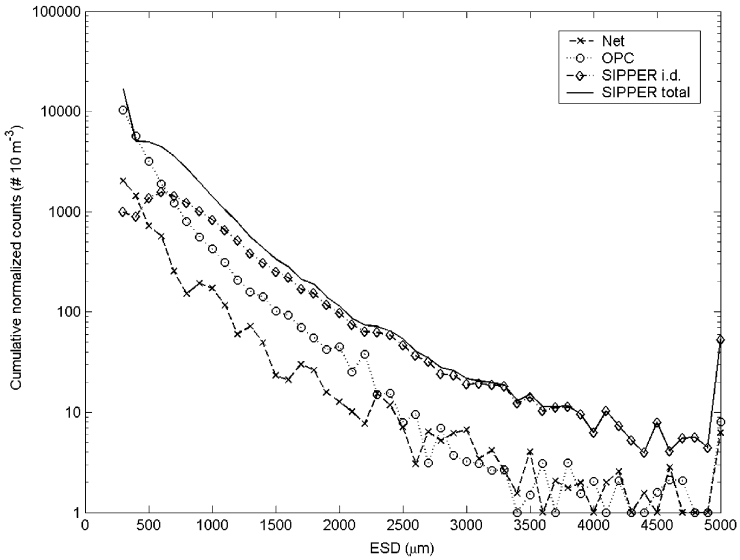

Fig. 7. Cumulative size-frequency distribution spectra for the three sampling sensors (300–5000 μm ESD). Data was normalized to volume filtered for each depth.

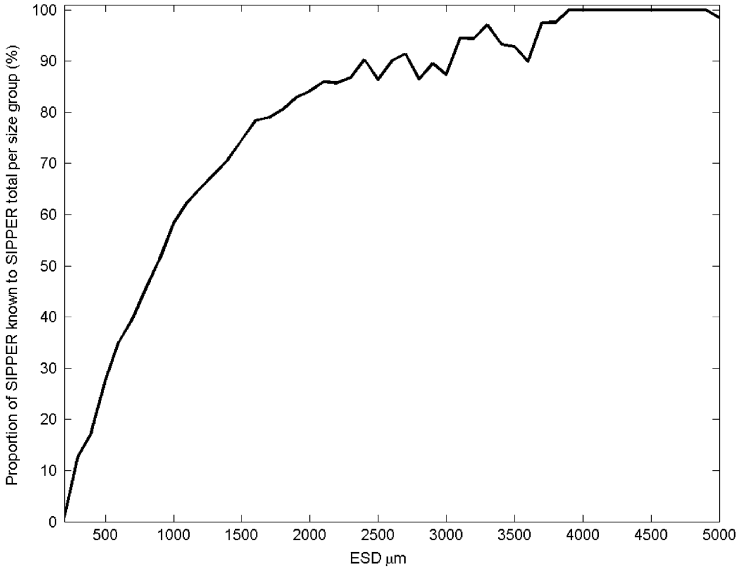

Fig. 8. Proportion of SIPPER identified plankton to the SIPPER image total per 100 μm ESD size class.

particles, the pixel size of 50 μm limits its ability to adequately describe small plankton organisms. Note that only 10 pixels would comprise the length of a 500 μm long organism, and therefore many small zooplankters were probably not identified as such in the SIPPER total dataset due to lack of resolvable characteristics. This concept is illustrated in a graph plotting the proportion of identifiable plankton images versus the SIPPER total (Fig. 8). This proportion rose

steadily with particle size, such that at ESDs over 2 mm, over 80% of the SIPPER ROIs were of identifiable plankton.

The inability of the OPC and nets to detect and sample the smallest size classes in the same magnitude as the SIPPER was most likely due to the inefficiency of the net in sampling the smallest zooplankton and suspended particulates due to extrusion through the net mesh (Gallienne et al., 2001; Hopcroft et al., 2001) and to approaching the 250 μm ESD detection limit for the OPC. Both the net and OPC additionally displayed a systematic abundance difference of up to an order of magnitude less at each size class compared to the SIPPER datasets, indicating that these differences were not size dependent.

3.5. SBV estimates

Differences in both the abundance and size distribution of the three datasets led to large differences in the SBV estimated by each sensor (Fig. 9). Because the main discrepancy in the SIPPER i.d. to SIPPER total abundance estimates was from the smallest size classes, the biovolume difference between the two was much less than the abundance difference due to the minimal contribution small particles or organisms make to the biovolume total. Thus, while the identified plankton of the SIPPER i.d. dataset made up only 28% of the SIPPER total particle abundance, they made up 79% of the SIPPER total biovolume. Net and OPC SBV were only 11% and 23% of the SIPPER total, respectively, and 13% and 29% of the SIPPER i.d. biovolume.

3.6. The problem of Trichodesmium

Ideally, the taxonomic composition of the net and SIPPER i.d. datasets should be identical. However, this was not the case, as the advantages and disadvantages of each system in sampling different components of the plankton were manifested in significantly different descriptions of the assemblage. Firstly, the colonial cyanobacteria *Trichodesmium* sp. formed the most abundant plankton class in the SIPPER dataset, especially at 10 m where it was found at concentrations greater than 1800 colonies m^{-3}, but were not quantified in the net samples. *Trichodesmium* is a

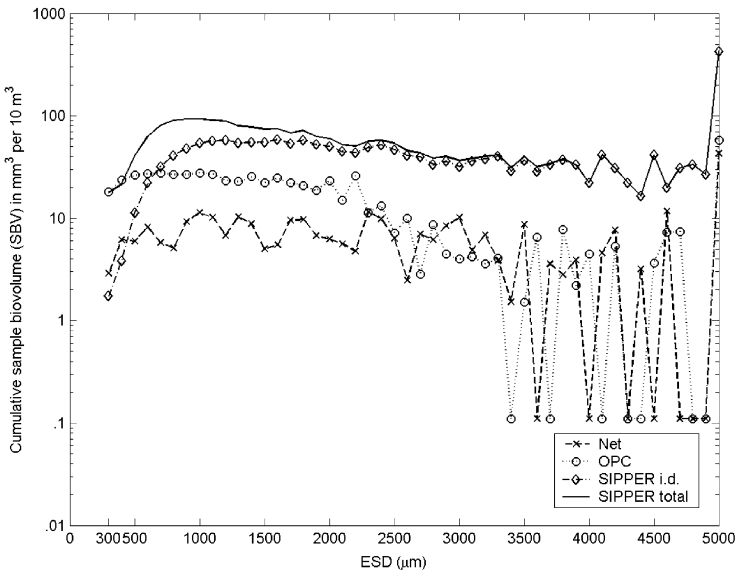

Fig. 9. Cumulative SBV (mm^3 $10\,m^{-3}$) versus size (300–5000 μm ESD) distribution. A logarithmic scale is used and the values transformed ($n + 0.1$).

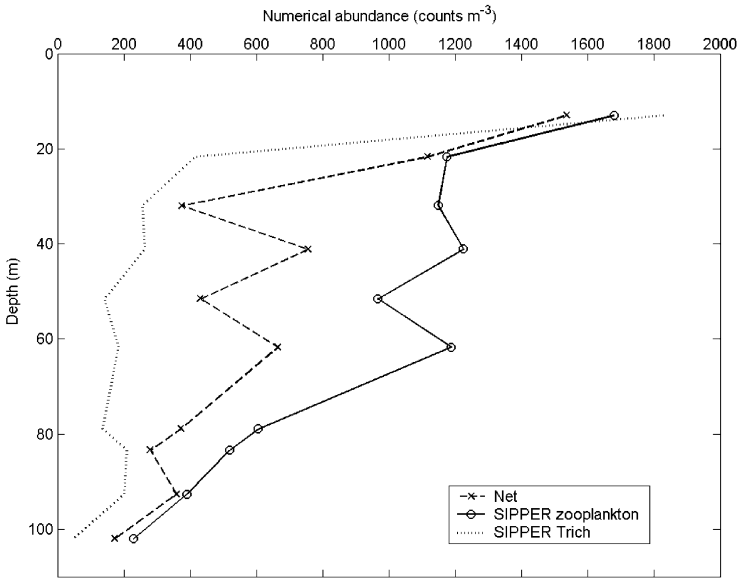

Fig. 10. Zooplankton abundance (numbers m^{-3}) profile determined from the net and SIPPER after *Trichodesmium* abundance was separated from the SIPPER i.d. dataset.

filamentous phytoplankton that is difficult to enumerate in zooplankton net samples because of its fragility and tendency to stick to the net mesh. The opacity and large size (0.5–4 mm ESD) of *Trichodesmium* colonies made them readily detectable by SIPPER and, most likely, the OPC. Those colonies that might have been fragmented or disrupted in the SIPPER sampling tube, and single trichomes (which image as long strands), were not counted as *Trichodesmium* in the SIPPER dataset. Removing the *Trichodesmium* images from the SIPPER i.d. dataset yielded zooplankton counts ~50% higher than that from the nets (Fig. 10).

3.7. Taxonomic composition—SIPPER vs. nets

The taxonomic composition of the zooplankton assemblage sampled by the two sampling methods varied even more considerably than the abundance. Data comparing zooplankton composition, abundance and biomass from the nets and SIPPER are presented in Tables 4 and 5, respectively. Copepods dominated the net samples, contributing 63.7% of the abundance and 36.4% of the biomass. Larvaceans (17.4%) were the only other significant contributor to the net abundance total, with the other tunicate class, comprising doliolids and salps, and the protoctista class, comprising mainly acantharians, radiolarians and tintinnids, contributing between 4% and 5% each. No other zooplankton class contributed more than 2.5% to the net-sample abundance total. Because of their large individual size, euphausiids and decapods were the second largest biomass component in the net samples, contributing slightly less (31.8%) than the copepods. Other crustaceans (comprising amphipods, cladocerans and ostracods), the other tunicates class, and siphonophores all contributed between 6% and 9% to the total net collected biomass, mostly based on their larger individual size. No other zooplankton group contributed more than 3.5% to the total biomass in the nets.

Six zooplankton groups were found to be significantly more abundant in the SIPPER i.d. dataset than the concurrent net estimates (Fig. 11a) according to paired *t*-tests (Zar, 1984). These taxa can be broadly grouped as fragile and or gelatinous zooplankton that are easily damaged

Table 4
Net estimated abundance (number m^{-3}) and biomass (mg m^{-3}) of zooplankton groups

Depth (m)	Chaetognath	Cnidarians and ctenophores	Copepod	Decapod and euphausiid	Other tunicates	Larvacean	Echinoderm plutei and bipinnaria	Mollusc	Other crustaceans	Polychaete[a]	Protoctista	Siphonophores[a]
10	19 (1.23)	4 (—)	1039 (13.15)	9 (6.73)	31 (3.39)	280 (0.99)	8 (0.01)	42 (0.62)	16 (1.70)	5 (0.01)	66 (NA)	17 (4.45)
20	15 (0.66)	5 (0.02)	775 (6.12)	3 (1.32)	15 (1.54)	161 (0.68)	4 (—)	63 (0.31)	13 (0.56)	2 (0.58)	51 (NA)	9 (0.81)
30	15 (0.7)	3 (0.02)	206 (2.65)	9 (12.12)	14 (0.43)	74 (0.31)	5 (—)	11 (0.14)	17 (1.92)	3 (0.01)	15 (NA)	5 (0.22)
40	22 (1.21)	3 (0.01)	462 (7.48)	8 (5.45)	24 (0.29)	159 (0.54)	3 (0.01)	6 (0.06)	21 (1.43)	1 (0.01)	37 (NA)	11 (0.73)
50	6 (0.94)	4 (0.02)	246 (5.36)	7 (1.19)	30 (0.37)	82 (0.29)	2 (—)	9 (0.18)	10 (0.49)	9 (0.28)	17 (NA)	10 (1.38)
60	8 (0.08)	4 (0.01)	289 (8.23)	3 (12.52)	133 (2.10)	162 (0.62)	3 (—)	14 (0.11)	18 (2.17)	2 (0.02)	21 (NA)	8 (0.63)
70	3 (0.17)	4 (0.01)	237 (2.99)	4 (0.53)	13 (0.52)	64 (0.21)	3 (—)	8 (0.04)	11 (0.93)	3 (0.01)	21 (NA)	3 (1.99)
80	4 (0.07)	3 (0.01)	199 (3.23)	2 (0.54)	4 (0.22)	41 (0.16)	2 (—)	2 (0.08)	9 (0.65)	4 (0.02)	8 (NA)	1 (0.02)
90	4 (0.10)	4 (0.01)	293 (2.88)	6 (6.00)	6 (0.11)	14 (0.05)	3 (—)	1 (0.05)	16 (2.41)	3 (0.01)	8 (NA)	2 (0.47)
100	2 (0.06)	2 (—)	121 (1.19)	3 (5.19)	1 (0.03)	16 (0.06)	8 (—)	—(—)	13 (1.24)	1 (—)	4 (NA)	1 (0.24)
Total	97 (5.21)	35 (1.24)	3866 (53.29)	54 (51.61)	271 (9.00)	1052 (3.92)	42 (0.04)	155 (1.59)	143 (13.49)	33 (0.94)	247 (NA)	65 (10.93)

'—' indicates less than 0.01 mg m^{-3}.
NA indicates biomass not determined for that group.
[a]indicates that body segments found in net counted as individuals.

Table 5
SIPPER estimated abundance (number m^{-3}) and biomass (mg m^{-3}) of zooplankton groups

Depth (m)	Chaetognath	Cnidarians and ctenophores	Copepod	Decapod and euphausiid	Other tunicates	Larvacean	Echinoderm plutei and bipinnaria	Mollusc	Other crustaceans	Polychaete	Protoctista	Siphonophores
10	22 (1.78)	117 (2.66)	537 (12.79)	11 (7.76)	81 (24.12)	608 (4.06)	16 (0.03)	16 (0.37)	16 (1.54)	5 (1.57)	257 (NA)	12 (3.7)
20	22 (1.75)	59 (2.11)	446 (7.58)	3 (2.77)	51 (11.89)	407 (3.37)	12 (0.02)	10 (0.11)	10 (1.24)	5 (0.97)	140 (NA)	23 (3.02)
30	27 (1.15)	73 (3.06)	258 (4.25)	13 (8.93)	122 (18.42)	466 (3.66)	8 (0.01)	9 (0.17)	15 (1.82)	4 (1.93)	145 (NA)	18 (3.93)
40	31 (0.89)	53 (0.75)	303 (7.90)	10 (5.27)	203 (18.95)	398 (2.83)	11 (0.02)	12 (0.09)	27 (3.10)	1 (0.17)	180 (NA)	7 (1.45)
50	8 (0.37)	50 (0.87)	284 (8.02)	4 (1.05)	180 (16.88)	265 (1.79)	10 (0.02)	13 (0.17)	14 (1.90)	5 (2.91)	137 (NA)	5 (0.63)
60	10 (0.37)	79 (1.01)	239 (8.61)	3 (8.39)	288 (19.20)	436 (2.77)	6 (0.02)	9 (0.12)	19 (2.50)	2 (1.14)	94 (NA)	10 (1.99)
70	9 (0.27)	32 (0.39)	195 (8.12)	3 (0.24)	61 (6.63)	173 (1.15)	3 (—)	5 (0.06)	9 (1.38)	1 (0.05)	112 (NA)	7 (1.05)
80	7 (0.43)	17 (1.06)	125 (3.65)	4 (1.53)	26 (1.99)	231 (1.36)	4 (—)	2 (0.25)	11 (2.16)	1 (0.43)	87 (NA)	8 (1.94)
90	7 (0.47)	17 (0.59)	88 (2.79)	3 (4.39)	12 (0.70)	143 (0.61)	6 (—)	4 (0.12)	11 (1.49)	1 (0.01)	83 (NA)	23 (6.48)
100	3 (0.10)	8 (0.35)	57 (1.32)	4 (6.31)	5 (0.17)	71 (0.36)	54 (0.04)	1 (0.01)	4 (1.78)	1 (0.21)	54 (NA)	22 (5.69)
Total	145 (7.59)	505 (12.85)	2532 (60.25)	56 (46.63)	1029 (119.07)	3199 (21.95)	130 (0.18)	80 (1.47)	135 (18.91)	23 (9.38)	1289 (NA)	134 (29.87)

'—' indicates less than 0.01 mg m^{-3}.
NA indicates biomass not determined for that group.

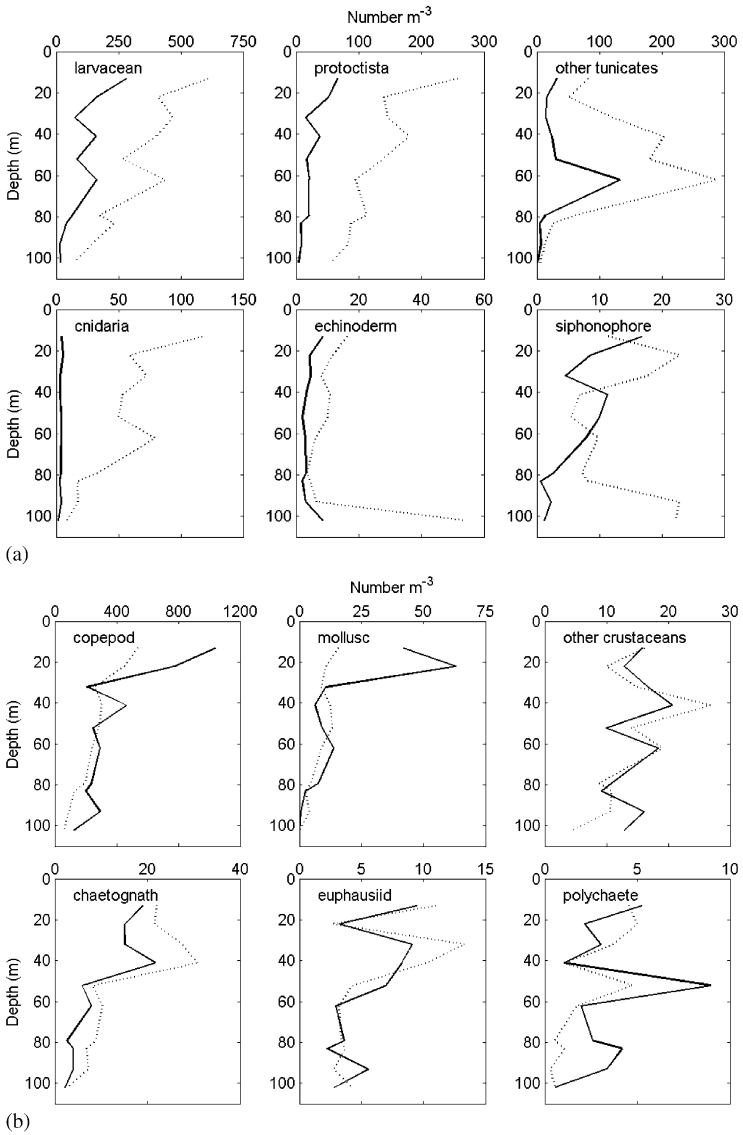

Fig. 11. (a) SIPPER (dotted line) and net (solid line) numerical abundance estimates of zooplankton groups with significant differences between the two sampling systems (paired t-test, $p<0.05$). (b) SIPPER (dotted line) and net (solid line) numerical abundance estimates of zooplankton groups with no significant differences between the two sampling systems ($p<0.05$).

or disrupted on encountering a net. These included 4 out of 5 of the most important numerical contributors to the SIPPER i.d. assemblage. Larvaceans were the numerical dominant, contributing 35.6% to the total and were more than $3\times$ more abundant than the net total. Three other fragile zooplankton groups (protoctista, other tunicates and cnidarians/ctenophores) were important numerically, each contributing between 5% and 14% to total zooplankton abundance. Copepods were the only important non-fragile zooplankton group and were the second highest contributor (27.7%) to the SIPPER i.d. abundance total. The differences in abundance between SIPPER and the nets for the fragile and gelatinous zooplankton ranged from just over, 200% for the

siphonophores to over 1400% for the cnidarians and ctenophores. However, the difference in siphonophore abundance was probably much higher, as individual bracts or nectophores found in net samples were counted as individuals whereas SIPPER imaged and counted whole organisms. This was also the case for polychaetes, which often were found broken up into segmented parts in the nets. The six other zooplankton groups, comprising mainly more robust taxa such as crustaceans, were sampled similarly by both the net and SIPPER and showed no appreciable difference in abundance (Fig. 11b).

Doliolids and salps, which made up the other tunicate class, were the biomass dominant in the SIPPER dataset, contributing 37% to the total. Examination of the SIPPER imagery and concurrent net data revealed that this group was dominated by *Dolioletta gegenbauri* or a similar congener, that made up more than 90% of the total. Interestingly, the large biomass difference (12.2 ×) between the SIPPER and net for this class was due not just to significant loss of individuals through the net mesh from extrusion or disruption (3.8 × more of this class were found in the SIPPER imagery), but also to loss of reproductive tissue. In the upper 60 m, a large proportion (33% mean, range: 22–39%) of the doliolids were of the asexually reproducing oozoid stage (Fig. 4L), which have a lengthened dorsal process or appendix that bears budding blastozooids that form the next stage in the doliolid life cycle. Very few doliolids observed in the net samples bore an intact dorsal process. Copepods (18%) and the euphausiids and decapod class (14%) each contributed over 10% to the SIPPER biomass total, while siphonophores (9%), larvaceans (7%) and other crustaceans (6%) contributed more than 5%.

Vertical distribution patterns of specific zooplankton groups sampled by both the nets and SIPPER were usually similar, even when the abundance estimates were quite different. For example, while doliolids and salps were significantly under-sampled by the nets compared to SIPPER, both instruments sampled an abundance maximum at the DCM much higher than at any other depth. However, for some zooplankton groups, SIPPER proved invaluable for describing both abundance and vertical distribution patterns that the nets did not resolve. For example, cnidarians and ctenophores were extremely abundant in the SIPPER dataset and demonstrated a strong bimodal distribution with maxima at 10 and 60 m, but were virtually absent within the net samples. Additionally, most cnidarians and ctenophores collected in nets are unidentifiable, especially after fixation. In contrast, within the SIPPER dataset, many individual cnidarian and ctenophore taxa could be enumerated to genus or even species. For example, we were able to determine that the narcomedusae *Solmundella bitentaculata* or a similar congener was the most abundant identifiable cnidarian in the depth ranges sampled.

3.8. Total biomass

Total biomass (0–100 m) determined from SIPPER data was more than twice that determined from the net data (3417 mg m^{-2} DW vs. 1592 mg m^{-2} DW), but the vertical biomass distribution pattern was similar. Most of the biomass difference was explained by the under representation of the fragile taxa in the net samples. The fragile and gelatinous zooplankton groups enumerated from the SIPPER dataset contributed greater biomass ($\sim$1937 mg m^{-2} DW) than the entire zooplankton assemblage sampled by the nets. Biomass did not include the protoctista class, which consisted of organisms with mineral skeletons or tests that may have biased the results. Because the protoctista class was more than 4 × more abundant in the SIPPER dataset than the nets, the true biomass difference was probably even greater.

3.9. Taxonomic differences in size distribution

Generally, the three sampling systems showed very little correspondence between particle abundance of a given size class (Fig. 12, left graphs), but some trends were apparent. Even though the absolute totals were very different, between 60% and 70% of the total net, OPC and SIPPER unidentified particle abundance consisted of

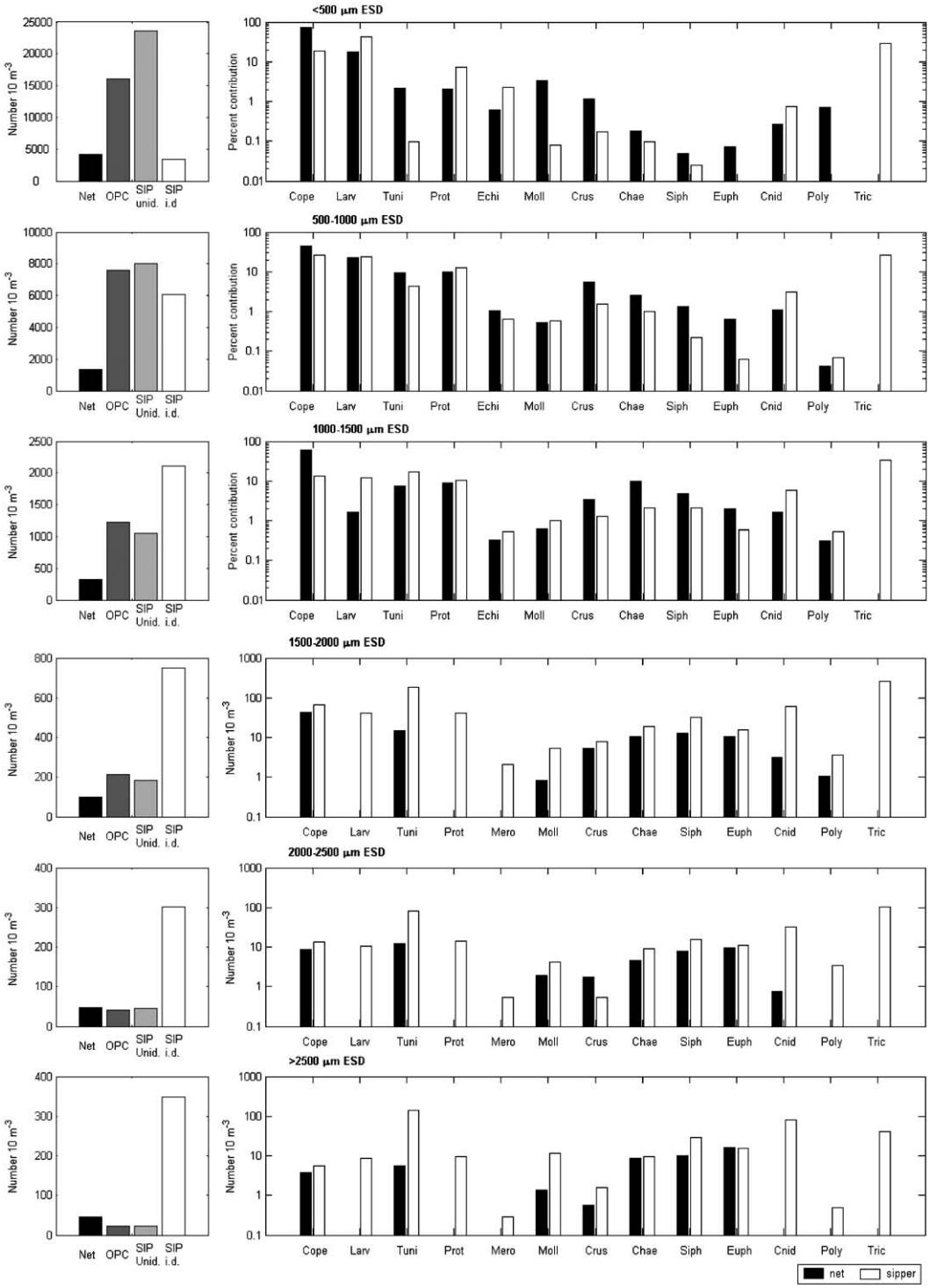

Fig. 12. Cumulative abundance of mesozooplankton sized particles or mesozooplankton determined by the three sampling methods separated into 500 μm size classes (left graphs). SIPPER data was separated into identified plankton and unidentified particles. Numerical abundance of the 13 plankton classes was calculated for each size class for the net samples and the SIPPER i.d. dataset (right graphs).

particles between 250 and 500 μm ESD and between 91% and 96% of the total were made up of particles less than 1 mm ESD. In contrast, only 73% of the SIPPER identified plankton were less than 1 mm ESD and the smallest size class contributed less than 26% of the total. The number of SIPPER identified plankton increased with size relative to the other three datasets. For example, SIPPER i.d. abundance at the largest size class (>2500 μm ESD) outnumbered nets, OPC and the SIPPER unidentified datasets by 6.8×, 7.5× and 15.5×, respectively.

Small zooplankton made up the majority of zooplankton sampled by both SIPPER and the nets, although the relative importance of larger forms was much greater in the SIPPER i.d. dataset (Fig. 12, right graphs). Whereas only 8.4% of the net collected zooplankton were larger than 1 mm ESD, more than 25% of the SIPPER imaged zooplankton were larger than this size. This difference was especially pronounced in the fragile and gelatinous zooplankton groups that were under sampled by the nets, such as the other tunicates class, where more than 74% of the SIPPER imaged organisms were larger than this size class compared to only 21% for those collected by the nets. However, this trend was also found for some of the zooplankton groups that showed no sampling bias in their abundance estimates. More than 90% of the net collected polychaetes were smaller than 0.5 mm ESD, while more than 80% of the SIPPER imaged polychaetes were larger than 1 mm ESD. Similarly for planktic mollusks, more than 95% of the net collected individuals were less than 1 mm ESD compared to only 47% for SIPPER.

4. Discussion

The disparate results between the three sampling methods is at first confusing given that the nets and the SIPPER sampled the exact same water volume and the OPC was sampling less than a meter away. This likely precludes the possibility that micro-scale patchiness affected these differences. The SIPPER provided a picture of a zooplankton assemblage both more numerous and diverse than either of the other methods. While the majority (~67%) of SIPPER extracted images could not be identified, those that were still significantly outnumbered organisms collected by the nets at most depths.

The number of unidentified particles in our dataset is comparable to that of other investigators using in situ imaging sensors. For example, Ashjian et al. (2001) were not able to classify 43% of VPR images collected during three cruises to Georges Bank. Additionally, they included marine snow as a class that comprised over 71% of their classified images. In contrast, we did not separate marine snow from our unclassified group. While many of these particle images were of identifiable marine snow such as cast-off larvacean houses, diatom rafts and fecal pellet strings, the majority of our unclassified images were of particles less than 1 mm ESD that lacked any resolvable characteristics to aid in identification. This was partly a problem of the imaging resolution of the SIPPER in that each pixel was approximately 50 μm square. A small copepodite or copepod nauplius measuring 400 μm TL would be imaged by the SIPPER but would be comprised of such a few number of pixels that identifying it as such is impossible with the present SIPPER configuration. Hopkins (1981), studying zooplankton at the same station as this study, found that metazoan plankton under 1 mm total length sampled from bottle casts outnumbered metazoan plankton >1 mm caught in a 162 μm plankton net by 35× and were made up primarily of copepod nauplii and copepodites. Thus, it is possible that a large percentage of the small-unidentified particles in the SIPPER dataset were of small zooplankton such as copepod early life stages. While we did not use data from the second camera of SIPPER for this study (which imaged orthogonal to the first), it may have assisted in identifying some of these smaller particles as well.

A substantial number of the larger classified images extracted from the SIPPER dataset were of *Trichodesmium* colonies, especially at 10 m where they outnumbered both the SIPPER and net zooplankton abundance estimates. *Trichodesmium* is an important component of tropical and subtropical oceanic ecosystems, contributing a

significant amount of new nitrogen to otherwise impoverished waters (Capone et al., 1997; Karl et al., 1997). Furthermore, *Trichodesmium* has been implicated in contributing to the initiation of harmful algal blooms of the dinoflagellate *Karenia brevis* (Lenes et al., 2001) in the Gulf of Mexico. Typically, the abundance and vertical distribution of *Trichodesmium* are determined with water bottles or drift nets, which are limited in their ability to detect it at low concentrations, can damage or distort specimens, and are prone to sampling error due to the small volumes sampled (Chang, 2000). Because SIPPER samples a larger volume of water, it can detect *Trichodesmium* at much lower concentrations than these traditional methods.

Other investigators using optical methods to investigate zooplankton distributions have also found that large colonial phytoplankton such as diatoms can dominate the marine particle assemblage within the mesozooplankton size range (Norrbin et al., 1996; Grant et al., 2000) The dominance of marine snow and of *Trichodesmium* and other phytoplankton in the water column suggests that data collected with non-imaging optical sensors such as the OPC must be interpreted with caution when converted to zooplankton abundance and size distributions. Imaging instruments such as the SIPPER, on the other hand, can separate these groups and allow for accurate determination of their contribution to the total marine particle assemblage.

There have been a number of studies investigating the performance of the OPC against plankton net catches (Sameoto et al., 1993; Grant et al., 2000; Halliday et al., 2001), but few if any comparisons against in situ imaging systems. Herman (1992) suggests that with strict sample and analysis control, net and OPC counts can agree to within 30%. Most studies, however, appear to have much more trouble reconciling the output of the OPC with what is collected within a net. Using the OPC mounted on the HRS to sample a 80 km transect on the West Florida Shelf, Sutton et al. (2001) found that the OPC grossly underestimated mesozooplankton abundance, especially at high concentrations ($>10{,}000$ organisms m^{-3}), but described the overall pattern of zooplankton fairly well. Herman (1988) and Sprules et al. (1998) have also reported OPC counts less than net counts, while others have reported large overestimates by the OPC relative to plankton nets (Grant et al., 2000; Halliday et al., 2001). Suggested causes of OPC underestimates are coincident counting (Sprules et al., 1992; Woodd-Walker et al., 2000; Labat et al., 2002) and the presence of highly translucent organisms (Wieland et al., 1997; Beaulieu et al., 1999), while overestimates have been attributed to the presence of marine snow and detrital aggregates (Zhang et al., 2000), large phytoplankton (Grant et al., 2000), small zooplankton that pass through the net mesh (Halliday et al., 2001; Zhou and Tande, 2002), and fragile organisms that are destroyed in the nets (Gallienne and Robins, 2001).

During this study, the OPC consistently sampled approximately half the number of particles that the SIPPER imaged at all depths. Much of this underestimation could have been due to coincidence, as we showed within the sub-sampled SIPPER imaging volume. More than 29% of the particles occurred within 4 mm of each other within the SIPPER "pseudovolume" and, therefore, would have been counted as a single particle if sampled by the OPC. By correcting for this, we were able to calculate OPC abundance estimates more in line with what SIPPER imaged in the mesozooplankton size range. The SIPPER data also showed that highly translucent forms such as cnidarians, ctenophores, doliolids and salps were important components in the zooplankton assemblage and may have partly explained the undercounting of larger particles by the OPC. While considerable effort was made to reduce the hydrodynamic presence of the sensors so as to reduce avoidance by active zooplankton, it is possible that there was a difference between the two sensors that could have contributed to the observed differences. Baumgartner (2003) found that late copepodite stages of *Calanus finmarchicus* could avoid the OPC at speeds similar to this study. Because the OPC has a wide but narrow sampling mouth (2×22 cm) and the SIPPER has a larger square aperture (9.6×9.6 cm), zooplankton may have been able to escape out of the way of the OPC more often than the SIPPER.

The deepwater Gulf of Mexico biological community has been sparsely sampled (Biggs and Ressler, 2001), but the general consensus is that the biology of offshore waters in the gulf is similar to that of other low-latitude tropical oceans, with low biomass and high diversity of zooplankton, ichthyoplankton and micronekton (Hopkins, 1981; Hopkins et al., 1996; Biggs and Ressler, 2001). The abundance, composition, size and vertical distribution and biomass of the mesozooplankton sampled during this study by the HRS plankton nets was similar to that found by one of us in an earlier study at this station (Hopkins, 1981) and to other investigations in oceanic waters of the Gulf of Mexico (Cummings, 1983; Ortner et al., 1989; Biggs and Ressler, 2001). Combined with an earlier study investigating the distribution of mesozooplankton on the West Florida Shelf using the HRS (Sutton et al., 2001), these results suggest that the somewhat small plankton nets used on the sampler provide similar results to those of other investigators using larger plankton nets to describe the mesozooplankton assemblage.

Comparing the HRS net catches versus what SIPPER imaged in the same water yielded a significantly different picture of the mesozooplankton assemblage. While a number of investigators have begun to stress the need to use multiple nets of different mesh sizes to adequately sample the entire mesozooplankton size range (Gallienne and Robins, 2001; Hopcroft et al., 2001), our results suggest that nets still might miss a large numerical and biomass fraction. Where copepods were both the numerical and biomass dominant in the net samples, larvaceans were the numerical dominant and doliolids and salps (forming the other tunicate class) were the biomass dominant in the SIPPER dataset. Small copepods, which made up the majority of the net-caught zooplankton, such as the genera *Calocalanus*, *Oithona*, *Paracalanus*, *Oncaea*, and *Temora,* were difficult to identify in the SIPPER dataset because of their small size even though they were most likely imaged, and therefore were underestimated (in this case counted in the SIPPER total). The large number of fragile and gelatinous organisms in the SIPPER dataset and their near absence in the nets obviously has implications on how a planktic ecosystem is described. For example, Hopkins et al. (1996) found that midwater shrimps and fish, the two dominant micronekton groups in this region, accounted for only 25% of the zooplankton daily production consumed in the eastern Gulf. It remains unresolved which ecosystem components are responsible for most zooplankton predation although they suspected large gelatinous predators. More work in this region with SIPPER might resolve that question.

Fixation of zooplankton samples with formalin has been shown to cause shrinkage of the preserved organisms (Postel et al., 2000). It is possible that shrinkage may have contributed to the observed differences between the size-frequency, biovolume and biomass of the net samples with that of the SIPPER. For example, Beaulieu et al. (1999) measured a 41% decrease in biovolume of the scyphozoan medusae *Aurelia aurita* and Nishikawa and Terazaki (1996) found that doliolids and salp body lengths shrank to approximately 86–93% of their live length after preservation. Omori (1978) observed that copepods and other crustaceans were less affected by fixation than gelatinous organisms. This likely explained some of the differences observed in the pteropod and polychaete size distribution in the net samples compared to SIPPER. However, the large differences in biovolume/biomass of the gelatinous and fragile organisms between SIPPER and the nets was due to increased abundance of these animals at all size classes. Therefore, the biovolume and biomass difference is due more to a difference in total abundance rather than a shift in the size frequency spectrum.

Prior investigations comparing net and imaging systems have yielded similar results to ours. Parallel deployments of the VPR and the MOCNESS on Georges Bank have shown that the MOCNESS significantly under-samples echinoderm larvae, larvaceans and medusae relative to the VPR (Benfield et al., 1996) and the VPR also sampled foraminifera, acantharians and other fragile protoctistan zooplankton more effectively than nets (Gallager et al., 1996; Norrbin et al., 1996; Ashjian et al., 2001). In those studies, however, copepods and other harder bodied organisms were still the numerical and biomass

dominant and thus the under-representation of the fragile forms appeared to be less important. In the central North Pacific Ocean, Dennett et al. (2002) reported that colonial radiolarian colonies averaged 380 × more abundant in VPR samples than those collected in the nets and were an important but overlooked component of biomass in oligotrophic waters. Similarly, our study in an oligotrophic central oceanic ecosystem indicated that traditional net sampling might miss more than half the mesozooplankton biomass.

This study demonstrates the importance of in situ imaging systems to accurately assess the abundance, size distribution and composition of a low-latitude mesozooplankton assemblage. The primary disadvantage of the SIPPER is the current need to manually classify the large volume of images generated by the sensor. The ability to automatically identify images of zooplankton collected in the lab or field has received considerable attention (Jeffries et al., 1984; Tang et al., 1998; Akiba and Kakui, 2000; Iwamoto et al., 2001) and an operable pattern recognition algorithm is in use for the VPR (Tang et al., 1998). We are currently developing an automated zooplankton classification system for the SIPPER to operate in near real-time while we continue to optimize the sensor. We have recently deployed a 2nd generation SIPPER with grayscale imaging and twice the resolution of the model used in this study. These improvements should allow us to discern and identify the smaller zooplankton such as small calanoid and poecilostomatoid copepods that were more abundant in the net samples and difficult to identify with the present SIPPER. With these advances we believe the SIPPER can provide more accurate mesozooplankton abundance and size measurements than nets and provide valuable insight into processes controlling zooplankton distributions at both the individual and community level.

Acknowledgements

We would like to thank the crew of the R/V *Suncoaster* of the Florida Institute of Oceanography for their excellent shipboard support. Additionally we would like to thank Dr. Tracey Sutton (HBOI) and Scott Burghart (USF College of Marine Science) for their assistance in the laboratory. We also would like to thank Mike Hall, Larry Langebrake, Jim Patten, Graham Tilbury and Joe Kolesar of the Center for Ocean Technology for their assistance in developing, deploying and maintaining the SIPPER. We would also like to thank Drs. Kendra Daly and John Walsh and two anonymous reviewers for their critical review of the manuscript. This work was funded by Office of Naval Research award no. N00014-96-1-5020.

References

Akiba, T., Kakui, Y., 2000. Design and testing of an underwater microscope and image processing system for the study of zooplankton distribution. IEEE Journal of Oceanic Engineering 25 (1), 97–104.

Ashjian, C.J., Davis, C.S., Gallager, S.M., Alatalo, P., 2001. Distribution of plankton, particles, and hydrographic features across Georges Bank described using the Video Plankton Recorder. Deep-Sea Research II 48 (1–3), 245–282.

Austin, H.M., Jones, J.I., 1974. Seasonal variation of physical oceanographic parameters on the Florida Middle Ground and their relation to zooplankton on the West Florida Shelf. Florida Scientist 37 (1), 5–16.

Baumgartner, M.F., 2003. Comparisons of *Calanus finmarchicus* fifth copepodite abundance estimates from nets and an optical plankton counter. Journal of Plankton Research 25 (7), 855–868.

Beaulieu, S.E., Mullin, M.M., Tang, V.T., Pyne, S.M., King, A.L., Twining, B.S., 1999. Using an optical plankton counter to determine the size distributions of preserved zooplankton samples. Journal of Plankton Research 21 (10), 1939–1956.

Benfield, M.C., Davis, C.S., Wiebe, P.H., Gallager, S.M., Lough, R.G., Copley, N.J., 1996. Video plankton recorder estimates of copepod, pteropod and larvacean distributions from a stratified region of Georges Bank with comparative measurements from a MOCNESS sampler. Deep-Sea Research II 43 (7–8), 1925–1945.

Biggs, D.C., Ressler, P.H., 2001. Distribution and abundance of phytoplankton, zooplankton, icthyoplankton and micronekton in the deepwater Gulf of Mexico. Gulf of Mexico Science 19, 7–29.

Capone, D.G., Zehr, D.G., Paerl, H.W., Bergmann, B., Carpenter, E.J., 1997. *Trichodesmium*, a globally significant marine cyanobacterium. Science 276, 1221–1229.

Chang, J., 2000. Precision of different methods used for estimating the abundance of the nitrogen-fixing marine

cyanobacterium, *Trichodesmium* Ehrenberg. Journal of Experimental Marine Biology and Ecology 245, 215–224.

Cummings, J.J., 1983. Habitat dimensions of calanoid copepods in the western Gulf of Mexico. Journal of Marine Research 41, 163–188.

Davis, C.S., Gallagher, S.M., Berman, M.S., Haury, L.R., Strickler, J.R., 1992. The Video Plankton Recorder (VPR): design and initial results. Archiv für Hydrobiologie—Advances in Limnology 36, 67–81.

Dennett, M.R., Caron, D.A., Michaels, A.F., Gallager, S.M., Davis, C.S., 2002. Video plankton recorder reveals high abundances of colonial Radiolaria in surface waters of the central North Pacific. Journal of Plankton Research 24 (8), 797–805.

Foote, K.G., 2000. Optical methods. In: Harris, R.P., Wiebe, P.H., Lenz, J., Skjoldal, H.-R., Huntley, M. (Eds.), ICES Zooplankton Methodology Manual. Academic Press, San Diego, pp. 259–295.

Gallager, S.M., Davis, C.S., Epstein, A.W., Solow, A., Beardsley, R.C., 1996. High-resolution observations of plankton spatial distributions correlated with hydrography in the Great South Channel, Georges Bank. Deep-Sea Research II 43 (7–8), 1627–1663.

Gallienne, C.P., Robins, D.B., 2001. Is *Oithona* the most important copepod in the world's oceans? Journal of Plankton Research 23 (12), 1421–1432.

Gallienne, C.P., Robins, D.B., Woodd-Walker, R.S., 2001. Abundance, distribution and size structure of zooplankton along a, 20° west meridional transect of the northeast Atlantic Ocean in July. Deep Sea Research II 48 (4–5), 925–949.

Grant, S., Ward, P., Murphy, E., Bone, D., Abbott, S., 2000. Field comparison of an LHPR net sampling system and an Optical Plankton Counter (OPC) in the Southern Ocean. Journal of Plankton Research 22 (4), 619–638.

Halliday, N.C., Coombs, S.H., Smith, 2001. A comparison of LHPR and OPC data from vertical distribution sampling of zooplankton in a Norwegian fjord. Sarsia 86 (2), 87–99.

Haury, L.R., McGowan, J.A., Wiebe, P.H., 1977. Patterns and processes in the time-space scales of plankton distributions. In: Steele, J.H. (Ed.), Spatial Patterns in Plankton Communities. Plenum Press, New York, pp. 277–326.

Herman, A.W., 1988. Simultaneous measurement of zooplankton and light attenuance with a new optical plankton counter. Continental Shelf Research 8 (2), 205–221.

Herman, A.W., 1992. Design and calibration of a new optical plankton counter capable of sizing small zooplankton. Deep Sea Research I 39 (3–4), 395–415.

Hopcroft, R., Roff, J., Chavez, F., 2001. Size paradigms in copepod communities: a re-examination. Hydrobiologia 453 (1–3), 133–141.

Hopkins, T.L., 1981. The vertical distribution of zooplankton in the eastern Gulf of Mexico. Deep-Sea Research 29 (9A), 1069–1083.

Hopkins, T.L., Sutton, T.T., Lancraft, T.M., 1996. The trophic structure and predation impact of a low latitude midwater fish assemblage. Progress in Oceanography 38, 205–239.

Iwamoto, S., Checkley, D.M., Trivendi, M.M., 2001. REFLICS: real-time flow imaging and classification system. Machine Vision and Applications 13, 1–13.

Jeffries, H.P., Berman, M.S., Poularikas, A.D., Katsinis, C., Melas, I., Sherman, K., Bivins, L., 1984. Automated sizing, counting and identification of zooplankton by pattern recognition. Marine Biology 378 (3), 329–334.

Karl, D.L.R., Tupas, L., Dore, J., Christian, J., Hebel, D., 1997. The role of nitrogen fixation in biogeochemical cycling in the subtropical North Pacific Ocean. Nature 388 (6642), 533–538.

Labat, J.M.P., Dallot, S., Errhif, A., Razouls, S., Sabini, S., 2002. Mesoscale distribution of zooplankton in the Sub-Antarctic Frontal system in the Indian part of the Southern Ocean: a comparison between optical plankton counter and net sampling. Deep-Sea Research I 49 (4), 735–749.

Lenes, J.M., Darrow, B.P., Cattrall, C., Heil, C.A., Callahan, M., Prospero, J.M., Bates, D.E., Fanning, K.A., Walsh, J.J., 2001. Iron fertilization and the *Trichodesmium* response on the West Florida Shelf. Limnology and Oceanography 46 (6), 1261–1277.

Lenz, J., 2000. Introduction. In: Harris, R.P., Wiebe, P.H., Lenz, J., Skjoldal, H.-R., Huntley, M. (Eds.), ICES Zooplankton Methodology Manual. Academic Press, San Diego, pp. 1–32.

Maul, G.A., Vukovich, F.M., 1993. The relationship between variations in the Gulf of Mexico Loop Current and Straits of Florida volume transport. Journal of Physical Oceanography 23, 785–796.

Müller-Karger, F.E., 2000. The spring 1998 Gulf of Mexico (NEGOM) cold water event: remote sensing evidence for upwelling and for eastward advection of Mississippi Water (or: how an errant loop current anticyclone took the NEGOM for a spin). Gulf of Mexico Science 19, 55–67.

Müller-Karger, F.E., Walsh, J.J., Evans, R.H., Meyers, M.B., 1991. On the seasonal phytoplankton concentration and sea surface temperature cycles of the Gulf of Mexico as determined by satellites. Journal of Geophysical Research 96 (C7), 12645–12665.

Nishikawa, J., Terazaki, M., 1996. Tissue shrinkage of two gelatinous zooplankton, *Thalia democratica* and *Dolioletta gegenbauri* (Tunicata: Thaliacea) in preservative. Bulletin of Plankton Society of Japan 43 (1), 1–7.

Norrbin, M.F., Davis, C.S., Gallagher, S.M., 1996. Differences in fine-scale structure and composition of zooplankton between mixed and stratified regions of Georges Bank. Deep Sea Research II 43 (7–8), 1905–1924.

Omori, M., 1978. Some factors affecting dry weight, organic weight and concentration of carbon and nitrogen in freshly prepared and preserved zooplankton. Internationale Revue der Gesamten Hydrobiologie 63, 261–269.

Omori, M.H., Hamner, W.M., 1982. Patchy distribution of zooplankton: behavior, population assessment and sampling problems. Marine Biology 72 (2), 193–200.

Ortner, P.B., Hill, L.C., Cummings, S.R., 1989. Zooplankton community structure and copepod species composition in

the northern Gulf of Mexico. Continental Shelf Research 9 (4), 387–402.

Ortner, P.B., Lee, T.N., Milne, P.J., Zika, R.G., Clarke, E., Podesta, G.P., Swart, P.K., Tester, P.A., Atkinson, L.P., Johnson, W.R., 1995. Mississippi River flood waters that reached the Gulf Stream. Journal of Geophysical Research 100 (C7), 13595–13601.

Postel, L., Fock, H., Hagen, W., 2000. Biomass and abundance. In: Harris, R.P., Wiebe, P.H., Lenz, J., Skjoldal, H.-R., Huntley, M. (Eds.), ICES Zooplankton Methodology Manual. Academic Press, San Diego, pp. 83–192.

Sameoto, D., Cochrane, N., Herman, A.W., 1993. Convergence of acoustic, optical, and net catch estimates of euphausiid abundance: use of artificial light to reduce net avoidance. Canadian Journal of Fishery and Aquatic Science 50, 334–346.

Samson, S., Hopkins, T., Remsen, A., Langebrake, L., Sutton, T., Patten, J., 2001. A system for high resolution zooplankton imaging. IEEE Journal of Oceanic Engineering 26 (4), 671–676.

Schulze, P.C., Williamson, C.E., Sprules, W.G., 1992. Concluding remarks: a comparison of new devices for studying zooplankton in situ. Archiv für Hydrobiologie—Advances in Limnology 36, 135–140.

Skjoldal, H.-R., Wiebe, P.H., Foote, K.G., 2000. Sampling and experimental design. In: Harris, R.P., Wiebe, P.H., Lenz, J., Skjoldal, H.-R., Huntley, M. (Eds.), ICES Zooplankton Methodology Manual. Academic Press, San Diego, pp. 33–54.

Sprules, W.G., Bergstrom, B., Cyr, H., Hargreaves, B.R., Kilham, S.S., MacIsaac, H.J., Matsushita, K., Stemberger, R.S., Williams, R., 1992. Non-video optical instruments for studying zooplankton distribution and abundance. Archiv für Hydrobiologie—Advances in Limnology 36, 45–58.

Sprules, W.G., Jin, E.H., Herman, A.W., Stockwell, J.D., 1998. Calibration of an optical plankton counter for use in fresh water. Limnology and Oceanography 43 (4), 726–733.

Sutton, T.T., Hopkins, T.L., Remsen, A., Burghart, S., 2001. Multisensor sampling of pelagic ecosystem variables in a coastal environment to estimate zooplankton grazing impact. Continental Shelf Research 21 (1), 69–87.

Tang, X., Stewart, W.K., Vincent, L., Huang, H., Marra, M., Gallager, S.M., Davis, C.S., 1998. Automatic plankton image recognition. Artificial Intelligence Review 12, 177–199.

Vidal, V.M.V., Vidal, F.V., Hernández, A.F., Meza, E., Zambrano, L., 1994. Winter Water Mass Distributions in the Western Gulf of Mexico affected by a colliding Anticyclonic Ring. Journal of Oceanography 50 (5), 559–588.

Warren, J.D., Stanton, T.K., Benfield, M.C., Wiebe, P.H., Chu, D., Sutor, M., 2001. In-situ measurements of acoustic target strengths of gas-bearing siphonophores. ICES Journal of Marine Science 58 (4), 740–749.

Wiebe, P.H., Benfield, M.C., 2003. From the Hensen net toward four-dimensional biological oceanography. Progress in Oceanography 56 (1), 7–136.

Wieland, K., Petersen, D., Schnack, D., 1997. Estimates of zooplankton abundance and size distribution with the Optical Plankton Counter (OPC). Archiv fur Fischerei- und Meeresforschung 45 (3), 271–280.

Woodd-Walker, R.S., Gallienne, C.P., Robins, D.B., 2000. A test model for optical plankton counter (OPC) coincidence and a comparison of OPC-derived and conventional measures of plankton abundance. Journal of Plankton Research 22 (3), 473–483.

Zar, J.H., 1984. Biostatistical Analysis. Prentice-Hall, Englewood Cliffs, NJ, pp. 1–718.

Zhang, X., Roman, M., Sanford, A., Lascara, C., Burgett, R., 2000. Can an optical plankton counter produce reasonable estimates of zooplankton abundance and biovolume in water with high detritus? Journal of Plankton Research 22 (1), 137–150.

Zhou, M., Tande, K., 2002. Optical Plankton Counter Workshop. GLOBEC Report 17, University of Tromso, Tromso.